

# Tribological Aspects of Cast Iron Investigated Via Fracture Toughness

C. Fragassa<sup>a</sup>, G. Minak<sup>a</sup>, A. Pavlovic<sup>a</sup>

<sup>a</sup>Department of Industrial Engineering, Alma Mater Studiorum University of Bologna, Italy.

## Keywords:

Compacted Graphite Iron (CGI)  
Spheroidal Graphite (SGI)  
Experimental analysis

## ABSTRACT

Linear-elastic plane-strain fracture toughness of metallic materials is a method which covers the determination of the strain fracture toughness ( $K_{Ic}$ ) of metallic materials by increasing-force test of fatigue precracked specimens. This method has been applied for investigating the fracture behaviour of cast iron. Two groups of cast alloys, Compacted Graphite Iron (CGI) and Spheroidal Graphite Iron (SGI) have been investigated. While SGI benefits of a wide scientific literature, CGI is a relatively unknown material despite of its large potentialities in industrial applications.

## Corresponding author:

Cristiano Fragassa  
University of Bologna,  
viale Risorgimento 2, Bologna, Italy  
E-mail: cristiano.fragassa@unibo.it

© 2016 Published by Faculty of Engineering

## 1. INTRODUCTION

Cast iron is a group of iron-carbon alloys with carbon content greater than 2 % [1]. The alloy constituents affect its colour when fractured. But, more relevantly, these constituents affect microstructure and final proprieties of the alloy. According to the microstructure (Fig. 1), the following families of cast alloy are conventionally identified [2]:

- white cast iron
- grey cast iron
- malleable cast iron
- ductile cast iron.



Fig. 1. Example of microstructures.

Actually, the only cast irons with significant commercial uses are the grey and the ductile ones. In fact, most of the production of white cast iron is intended for a further reprocessing aimed at obtaining malleable or ductile cast irons. At the same time, the malleable cast iron is declining very fast since its processing presents a higher complexity, not justified by lower improvements in the mechanical proprieties.

Comparing grey and ductile cast irons, even if the grey is largely used nowadays, it is mainly limited to “technically pour” applications where the lowest cost appears one of the main advantages driving this material selection. On the contrary, ductile cast iron uses to represent the “preferable choice” wherever superior mechanical characteristics are requested. Several interesting dissertations are available with the aim at comparing the proprieties [3-5] or in specific the fields of applicability [6,7] of these different cast alloys.

In general, it is possible to summarize reporting that ductile cast iron offers an incredibly high mechanical propriety thanks to the spheroidal shape of graphite in the alloy. Their presence is so relevant for the final proprieties that this material is also known worldwide as *Spherical Graphite Iron* (SGI) or *Nodular cast iron* [8].

In was produced for the first time in 1943, where a ladle addition of magnesium (as a copper-magnesium alloy) to cast iron was made. It was noticed that the solidified castings contained not flakes, but nearly perfect spheres of graphite. These spheres don't act as stress raisers, but as crack arresters offering to the iron its ductility. This new form of cast iron immediately found uses where malleable iron, forgings, cast steel or steel fabrications would have been used [9].

Technological advantages of SGI are numerous providing its success [10-12]. They can be summarized as versatility and higher performance at lower cost. Other members of the ferrous casting family may have individual properties which might make them the material of choice in some applications, but none have the versatility of SGI, which often provides the designer with the best combination of overall properties (Fig. 2). This versatility is especially evident in the area of mechanical properties where Ductile Iron offers the designer the option of choosing high ductility, with grades guaranteeing more than 18% elongation, or high strength, with tensile strengths exceeding 825 MPa.

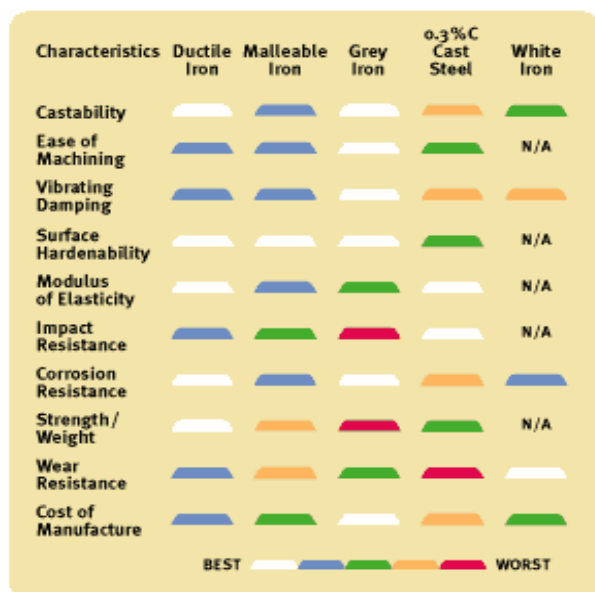


Fig. 2. Comparing different forms of cast iron.

Almost in the same period, other specific modifications in foundry process permitted to realize the so called *Compacted Graphite Iron* (CGI) or *Vermicular Graphite Iron*. Also in the case of CGI, its peculiarities are in net relation with the specific shape of the graphite particles (Fig. 3). While grey cast iron is characterized by randomly oriented graphite flakes and in ductile iron (SGI) graphite exists as individual spheres, in CGI graphite flakes are randomly oriented and elongated as in grey iron, but they are shorter, thicker and with rounded edges, in some aspects more similarly to SGI [13].

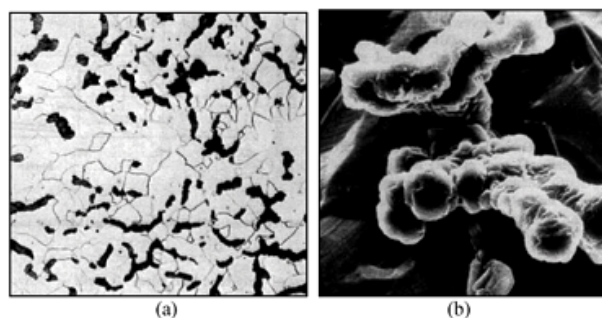


Fig. 3. Microstructure of Compacted Graphite Iron: a) optical micrograph; b) 3-D shape [14].

But, at least considering the main mechanical proprieties, CGI appeared significantly inferior respect to SGI: it is possible to say that SGI is twice as strong as CGI. And even referring to the production, the process is more complex than in the case of CGI, so that the stable production range for SGI is five times larger. These limits regarding material and process represent the reason why, up to now, the CGI has had a very restricted penetration in the market (Tab. 1).

But several limitations in the use of grey or ductile cast iron for modern applications are evident. And, in a future perspective, the Compacted Graphite Iron can be a valid solution. Although stronger and easier to produce respect to CGI, the choice between grey and ductile iron forced designers to select from either end of the cast iron spectrum: grey iron with good castability, machinability, damping capacity and thermal conductivity; or, ductile iron with good strength and stiffness. But, most applications required a compromise. With better strength and stiffness than grey iron, and better castability, machinability and thermal conductivity than ductile iron, CGI is ideal for components with simultaneous mechanical and thermal loading, such as cylinder blocks and heads [15].

**Table 1.** Typical properties of grey, compacted and ductile cast irons [13,16,17].

Propriety		Grey	CGI	SGI
Tensile Strength	MPa	250	450	750
Elastic Modulus	GPa	105	145	160
Elongation	%	0	1.5	5
Thermal Conductivity	W/mK	48	37	28
Damping Capacity		1	0.35	0.22
R-B Fatigue	MPa	110	200	250
Hardness	BHN	190	230	235

For the sake of completeness, it is possible to report that grey, spheroidal or white cast irons can present interesting changes in proprieties when their alloys are “powered” including elements, such as nickel, molybdenum, silicon, chromium, or copper, with more than 3 % as concentration. For instance, including these specific element in the alloy, it is possible to enlarge the applicability of cast iron even to include special cases, where high resistance to deformations [18], wear [19], corrosion [20], oxidation or to temperatures are required. Moreover, changing the compositions, the alloys can be particularly suitable for castings which have to be in contact with sea water, oils, acids or salts, for the chemical industry, oil industry, food industry or shipbuilding [21-23].

## 2. MATERIALS

In this investigation, 14 specimens were tested. The specimens were extracted from CGI and SGI green sand cast plates taken from two different production batches.

Specifically, during the first part of specimens’ production, a plate in SGI and, just later, a plate in CGI were casted. They were realized inside the same process and using, as base, the same melting alloy, but modifying the composition by inclusion of additives. In practice, specific and different additives were directly introduced in the furnace to produce SGI or CG [24,25].

Six weeks later, the same process was implemented with the aim at realising a second set of specimens.

Special attentions were adopted to keep the same operative conditions utilized in the previous stage of production. In this way, the repeatability of the melting process, that uses to

involve about 30 % of ferrous scrap and a cupola furnace, was also checked.

Regarding the additives, in the case of SGI castings, before the pouring, the melt (with a sulphur content lower than 0.01% wt.) was inoculated by adding ferrosilicon alloys and modified with *Fe-Si-Mg* master alloys. In the production of CGI castings also Ti was added. In all cases, the pouring temperature was 1400°C. A specific thermal analysis provided immediate feedbacks reporting the chemical composition of melting alloy after the inoculation of additives (Fig 4). This in-process test permits a constant regulation on additives and a better control on the final composition.

A deeper analysis, using optical and scanning electron microscopy (Fig. 5), was also carried out according to ASTM A247 [26].

Table 2 reports the chemical compositions of specimens and gives evidence of the different in microstructures between the two materials.



**Fig. 4.** Sample taking from ladle permitting a thermal analysis with the aim at obtaining the chemical composition of alloy after the inoculation of additives (Courtesy SCM Group).

**Table 2.** Chemical composition for 1<sup>st</sup> and 2<sup>nd</sup> batch specimens.

Elements	C	Si	Mn	P	S	Ni	Cr	Cu	Mg	Sn	Ti	Al
SGI (1 <sup>st</sup> batch)	3.66	2.6	0.218	0.032	0.004	0.069	0.062	0.052	0.055	0.013	0.034	0.011
SGI (2 <sup>nd</sup> batch)	3.63	2.65	0.276	0.036	0.002	0.06	0.083	0.077	0.049	0.011	0.033	0.011
CGI (1 <sup>st</sup> batch)	3.68	2.67	0.215	0.029	0.007	0.068	0.061	0.05	0.014	0.013	0.073	0.01
CGI (2 <sup>nd</sup> batch)	3.63	2.57	0.272	0.034	0.005	0.06	0.082	0.075	0.012	0.011	0.074	0.011

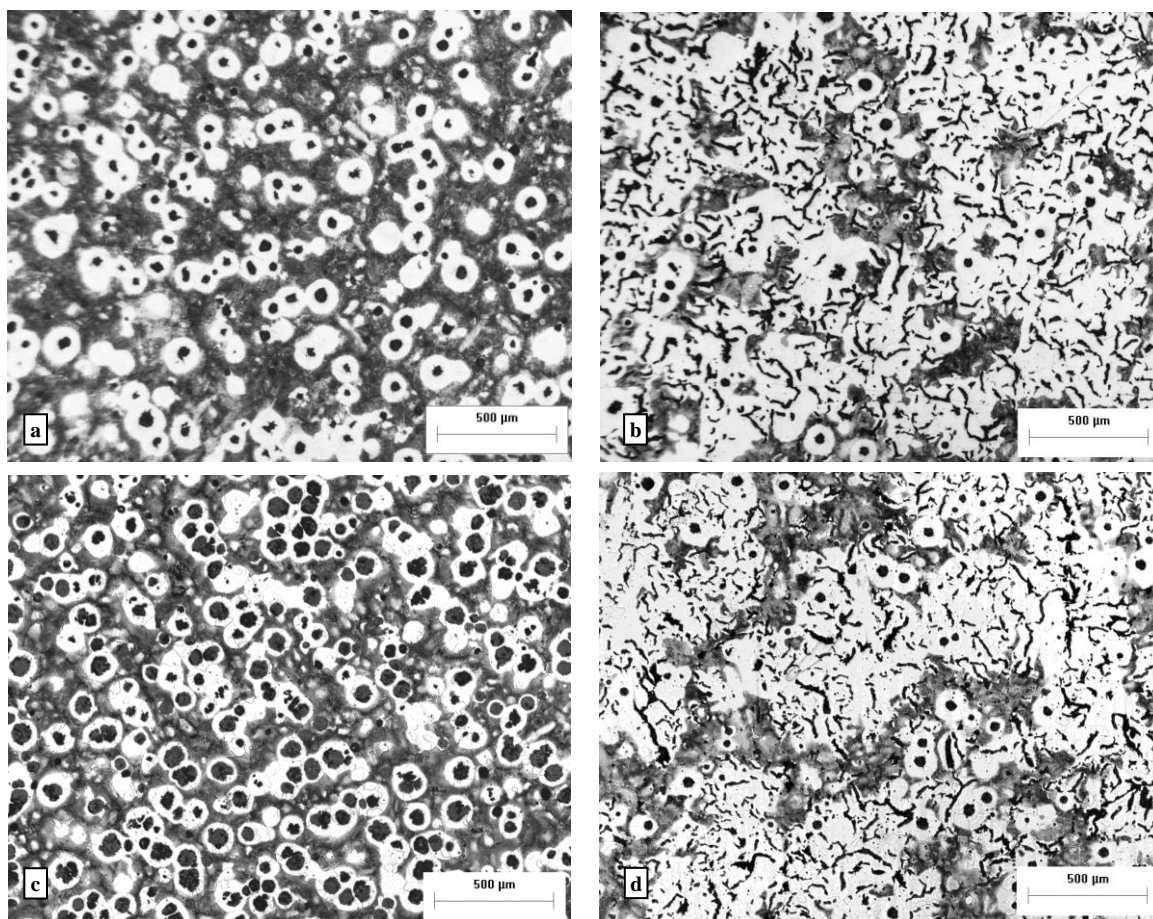


**Fig. 5.** OM micrographs after Nital etching of: 1st batch SGI specimen (a); 1st batch CGI specimen (b); 2nd batch SGI specimen (c); 2nd batch CGI specimen (d). Graphite nodules and worms (black), ferrite islands (white) and perlite (grey) are evident.

### 3. METHODS

Fracture Toughness Testing measures the conditions under which an existing crack in a material will extend. Fracture toughness is an important material property in design applications since the occurrence of flaws is not completely avoidable. Flaws may appear as cracks, voids, inclusions, weld defects or design discontinuities. The Fracture Toughness Test is also valuable in determining whether there is a danger of component failure when a flaw is discovered in an existing structure. In the current experiment, tests were realized in accordance with ASTM E399 and ASTM E1820. Both standards are largely used in testing Fracture Toughness. Both of

them requires a precisely machined specimen, prepared with an EDM notch, and a specific equipment for bending tests.

On the contrary, these standards present relevant differences especially in the way of application of loads:

- ASTM E399 applies a continuously increasing load to the specimen and determines  $K_{IC}$  [27].
- ASTM E1820 applies a rising load with periodic partial unloading, measure the instantaneous crack length, providing  $K_{IC}$ ,  $KJ_{IC}$  and  $J_{IC}$  [28].

Crack-Tip Opening Displacement (CTOD) is also available from the data analysis. According to these standards and large part of the technical literature [29], the stress-intensity factor, namely “K”, is used to characterize the fracture toughness of linear elastic materials, which are typically high strength materials that fail in a brittle manner. The “J” integral describes elastic-plastic fracture toughness in more ductile materials which are better able to deform and resist crack growth under load. A Roman numeral subscript added to “K” and “J” indicates which of the three modes of fracture is used in the test. Mode I fracture is most common and is the condition in which a tensile load is applied normal to the direction of the crack plane. When a cracked material under Mode I plane-strain conditions reaches a critical value, denoted as  $K_{IC}$  or  $J_{IC}$ , the crack will begin to grow.

Inside these standards it is possible to find the general recommendations and requirements for  $K_{IC}$  testing. In their annexes specific information is also available on specimens (Fig. 6) and specimen configurations, displacement gage, loading fixture design (Fig. 7), together with a detailed procedure for fatigue pre-cracking. When materials behaves in a linear elastic manner prior to failure, such that the plastic zone is small compared to specimen dimensions, a critical value of the stress intensity factor,  $K_{IC}$ , may be an appropriate fracture parameter.

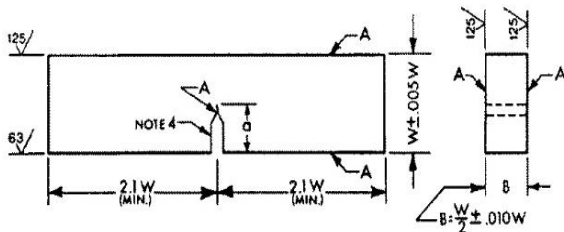


Fig. 6. Bend specimen with an EDM notch (ASTM 399).

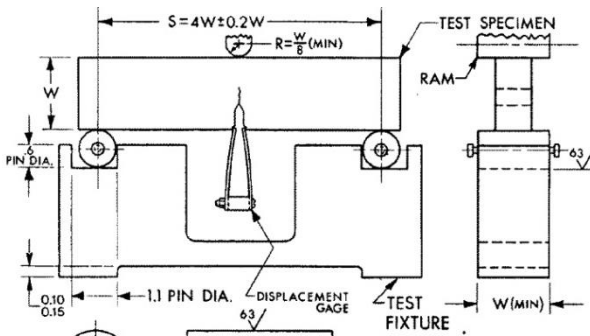


Fig. 7. Bend test fixture design (ASTM 399).

#### 4. TESTS

Fracture Toughness tests were performed on N. 14 specimens (Fig. 8). The bending force was increased until the specimens could not sustain further increase in load. This value is  $P_{MAX}$ .

The loading rate was chosen saving a condition of quasi-static tests: the rate of increase of stress-intensity factor in specimens was around  $2 \text{ MPa}\sqrt{m/s}$  during the initial elastic displacement. The standard permitted to evaluate the loading rate corresponding to this upper limit in the stress-intensity factor rate.

It was also verified that the plane of the fatigue precrack and subsequent 2 % crack extension (in the central flat fracture area; that is, excluding surface shear lips) was parallel to the plane of the starter notch to  $\pm 10^\circ$ . Adding, there was no evidence of multiple cracks.

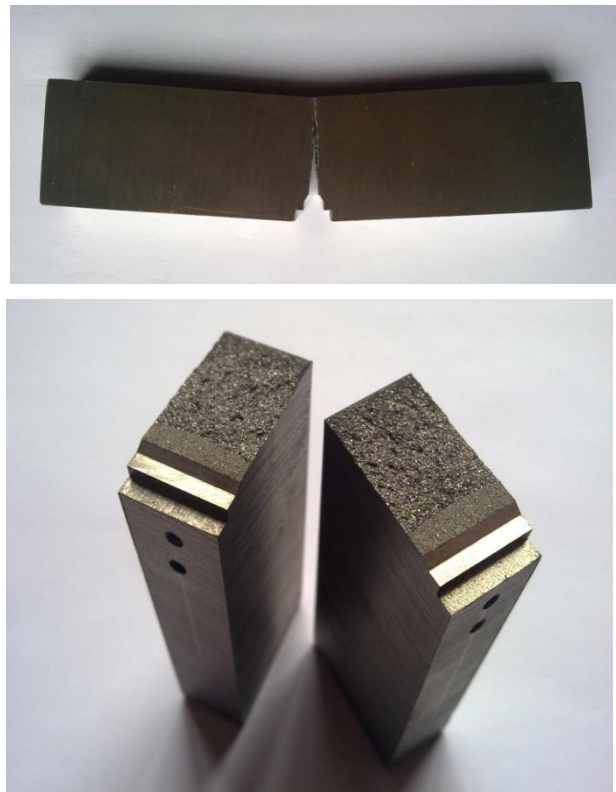
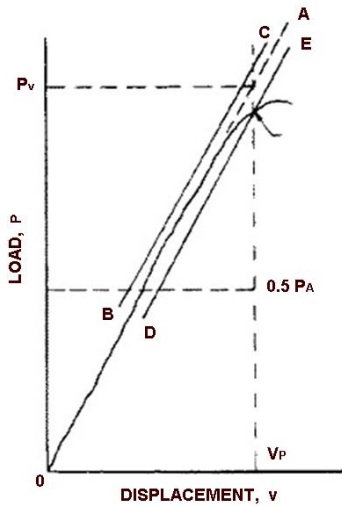


Fig. 8. specimen after breaking.

The force,  $P_0$ , at a 5 % secant offset from the initial slope, corresponding to about 2.0 % apparent crack extension, was established by a specified deviation from the linear portion of each graph (Fig. 9). The value of  $K_{IC}$  was calculated from this force using specific parameterized equations (see below).



**Fig. 9.** Method for analysis of load vs displacement graph (while  $P_Q$  is visible, 5 % secant line not shown).

In each test, a curve representing loads vs displacements was evaluated and used to substantiate the validity of the  $K_{IC}$  determination. This method passes by the evaluation of the “conditional result”,  $K_Q$ , that determines whether the result is consistent with the size and yield strength of the specimen. Between the other conditions for the correct application of ASTM E399, the ratio  $P_{MAX}/P_Q$  has not to exceed the value of 1,10, as recorded, for instance, in the case of *specimen 68* (Fig. 10).

$$\frac{P_{max}}{P_Q} = \frac{19800}{18800} = 1.05 < 1.1 \quad (1)$$

In this case,  $K_Q$  and  $K_{IC}$  could be coincident.

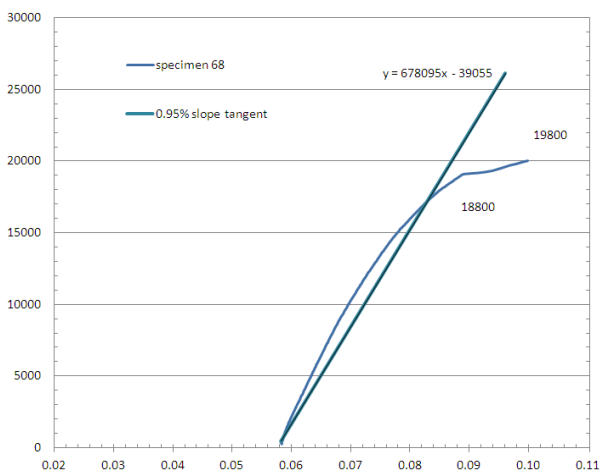


**Fig. 10.** Procedure for obtaining  $P_Q$  (ASTM E1820)

Otherwise, ASTM E1820 with rising loads and periodic partial unloading has to be preferred. When ASTM E1820 is used, two ASTM standards currently address the evaluation of experimental

data. In particular, the ASTM E813 standard outlines a test method for estimating the critical Resistant Curve,  $J$ , near initiation of ductile crack growth [30]. It divides  $J$  into elastic and plastic components and considers:  $J = J_{el} + J_{pl}$

$$J_{el} = \frac{K^2(1-\nu^2)}{E} \quad (2)$$

$$J_{pl} = \frac{2A_{pl}}{Bb_0} \quad (3)$$

where  $K$ ,  $E$ ,  $\nu$  represent materials properties,  $B$ ,  $b_0$  represent dimensions of specimens and  $A_{pl}$  area is shown in Fig. 11.

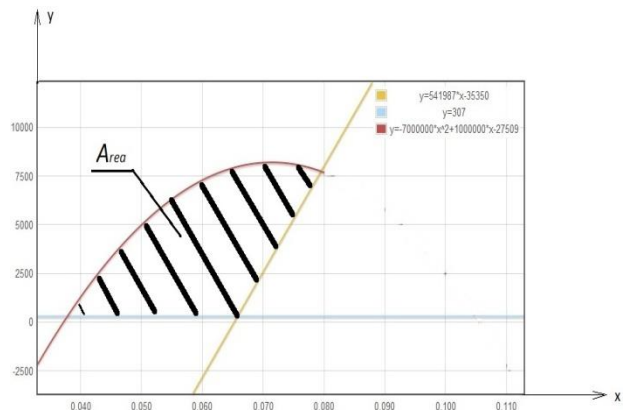


**Fig. 11.** Procedure for  $J$  calculation (ASTM E813)

The application of ASTM E1820 and ASTM E813, as shown in Fig. 12, is mandatory, for instance, for *specimen 29* considering that, in this case:

$$\frac{P_{max}}{P_Q} = \frac{14795}{10343} = 1.43 > 1.1 \quad (4)$$

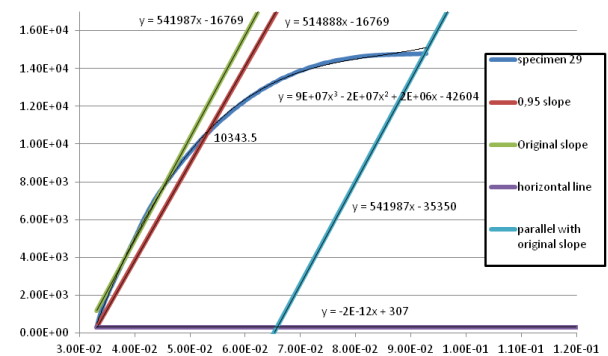


**Fig. 12.** Procedure for  $J$  calculation (ASTM E1820).

It is noteworthy that, in this investigation, specimens represented 4 different groups (exactly SGI or CGI and 1<sup>st</sup> or 2<sup>nd</sup> batch). Each group has a consistency between 3 and 5 samples, not permitting the general coincidence between  $K_Q$  and  $K_{IC}$  over the groups,

independently by specific value assumed for each specimen by the ratio  $P_{MAX}/P_Q$ .

As a consequence,  $K_Q$  instead of  $K_{IC}$  was evaluated, while criteria from both ASTM 399 or 1820 were used during the analysis.

### 5. PARAMETERS

Without entering in details of formula used for the estimation of the *fracture toughness* by ASTM 399 or 1820, it is convenient to highlight that measurements essential to the calculation of  $K_Q$  (or  $K_{IC}$ ) and  $V_m$  (CTOD) are specimen thickness  $B$ , crack size  $a$ , and width  $W$ .

Accordingly to the standards, Thickness [ $B$ ] was measured before testing to the nearest  $0.03\text{ mm}$  or to  $0.1\%$  whichever is larger. For plain-sided specimens,  $B$  was measured adjacent the notch. Width [ $W$ ] was measured, in conformance with the procedure appropriate to the specimen configuration, to the nearest  $0.03\text{ mm}$  or to  $0.1\%$  whichever is larger, at not less than three positions near the notch location, and the average value recorded. Specimen crack size [ $a$ ] was measured after fracture to the nearest  $0.5\%$  at mid-thickness and the two quarter-thickness points. The average of these three measurements was taken as the crack size,  $a$ . The difference between any two of the three crack size measurements was checked and verified as not exceeding  $10\%$  of the average. The crack size was measured also at each surface. For the straight-through notch starter configuration, no part of the crack front was closer to the machined starter notch than  $0.025W$  or  $1.3\text{ mm}$ , whichever was larger, furthermore, neither surface crack size measurement was differ from the average crack size by more than  $15\%$  and their difference did not exceed  $10\%$  of the average crack size.

These relations were used:

$$a_{initial} = a_0 \tag{5}$$

$$a_{avg.} = (a^{1/4} + a^{2/4} + a^{1/2})/3 \tag{6}$$

where:

$a^{1/4}$  = crack size at the  $1/4$  distance from the left side

$a^{2/4}$  = crack size at the  $1/4$  distance from the right side

$a^{1/2}$  = crack size at the  $1/2$  distance

then is:

$$a = a_{avg.} + a_{initial} \tag{3}$$

The overall representation of these dimensional parameters in a cracked sample is reported in Fig 13.

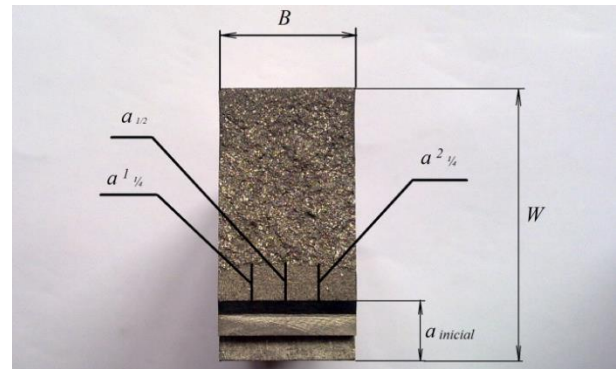


Fig. 13. One specimen after breaking

### 6. RESULTS

The Linear-elastic plane-strain fracture toughness of specimens in SGI and CGI is reported, respectively, in Tab. 3 and 4 in terms of  $K_Q$  [ $\text{MPa}\sqrt{\text{m}}$ ] and  $V_m$  [ $\text{mm}$ ].

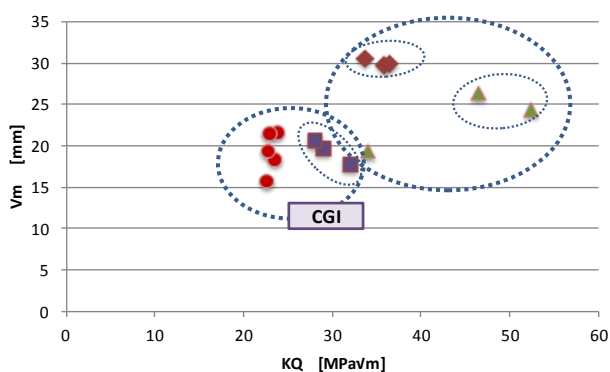
$K_Q$  and  $V_m$  are also graphically exposed in Fig. 14 showing the way these values are grouped in respect of alloy and batch. Even if experiments reported a slight variability in measures between the 1<sup>st</sup> and 2<sup>st</sup> batch, (for instance, around  $25\%$  for  $K_Q$  and  $30\%$  for  $V_m$  in the case of SGI), several general considerations are possible.

Table 3. Fracture Toughness of SGI.

SGI (Spheroidal Graphite Iron)		
Specimen	$K_Q$ [ $\text{MPa}\sqrt{\text{m}}$ ]	$V_m$ [ $\text{mm}$ ]
spec. 68	52.3	24.536
spec. 72	33.9	19.431
spec. 73	46.3	26.509
Average	<b>44.2</b>	<b>23.492</b>
St.Dev.	<b>9.37</b>	<b>3.653</b>
spec. 158	35.6	29.965
spec. 161	33.6	30.807
spec. 163	36.3	30.132
Average	<b>35.2</b>	<b>30.301</b>
St.Dev.	<b>1.4</b>	<b>0.446</b>

**Table 4.** Fracture Toughness of CGI.

CGI (Compacted Graphite Iron)		
Specimen	$K_Q$ [MPa√m]	$V_m$ [mm]
spec. 27	28.8	19.745
spec. 28	27.9	20.813
spec. 29	31.8	17.893
<i>Average</i>	<b>29.5</b>	<b>19.483</b>
<i>St.Dev.</i>	<b>2.04</b>	<b>1.47</b>
spec. 111	23.6	21.828
spec. 113	22.7	21.592
spec. 114	22.4	15.832
spec. 115	23.4	18.426
spec. 117	22.6	19.503
<i>Average:</i>	<b>22.9</b>	<b>19.436</b>
<i>St. Dev.:</i>	<b>0.53</b>	<b>2.469</b>



**Fig. 14.** Fracture Toughness of SGI and CGI in terms of  $K_Q$  [MPa√m] and  $V_m$  [mm].

SGI presents, respect to CGI, a superior ability to resist fracture as expressed by the higher values of the stress intensity factors ( $K_Q$ ) at which a crack begins to grow (also reported by [31]). This propriety can be also referred by the higher values in the plastic-elastic energy required to grow a crack ( $J_{Ic}$ ). But, it also means that SGI undergoes to ductile fracture (instead of a brittle one), in line with higher values in the Crack-Tip Opening Displacement ( $V_m$ ).

In Fig 15 the fracture surfaces of both cast irons are reported by SEM micrographs. It is clear how cleavage is the dominant fracture mechanism. At the same time, CGI showed higher decohesion at the matrix-graphite interface resulting in lower ductility. In fact, in CGI specimens, cleavage planes are wider and with very high decohesion at the matrix-graphite interface. It can be seen as

a reason for the CGI lower ductility and different plastic behaviour. An additional explanation can be found in the different hardness respect to SGI due to the dissimilar perlitic fractions of the matrices of the two materials. These evaluations are in accordance with [32].

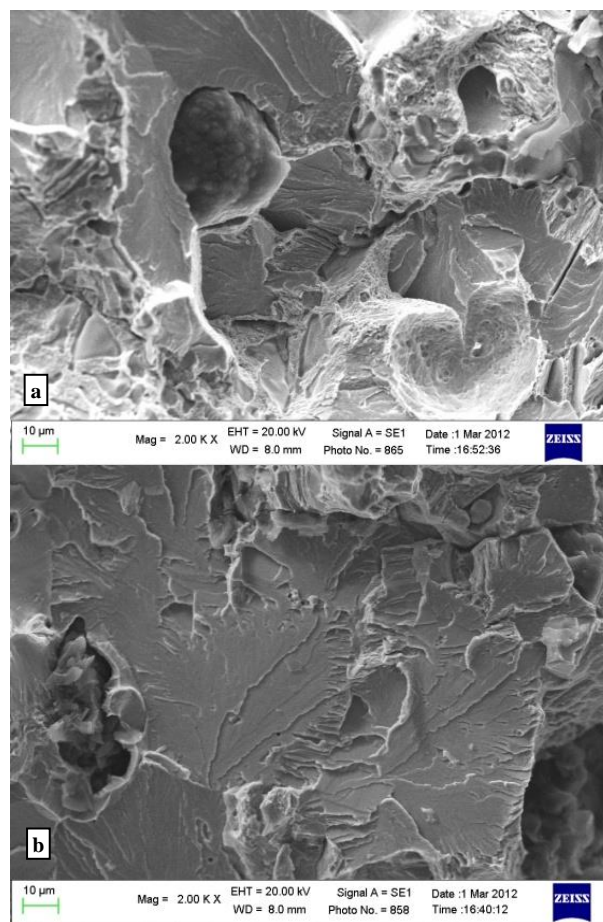


**Fig. 15.** High magnification SEM micrographs on the fracture surfaces of SGI (a) and CGI (b) specimens.

Referring to the modification of mechanical proprieties between different lots of production, it is evident how, while CGI seemed to preserve a very similar behaviour, SGI proved a larger variability. It can be explained by the dissimilar microstructure of specimens. Besides the same grade of nodularity, due to a similar  $Mg$  content inoculated in the alloy (Tab. 3), specimens extracted from SGI 1<sup>st</sup> batch were characterised (respect to the 2<sup>nd</sup> batch) by a lower graphite content, a slightly higher nodule density and a lower average nodule area. Furthermore, they seems to have higher content of perlite and lower of ferrite. This difference is due to small changes in the chemical compositions of the two batches of SGI with impact even on hardness. These considerations are also in line with [33].

## 7. CONCLUSION

In this analysis Fracture Toughness measures were realized with the aim at investigating the fracture behaviour of two families of cast alloys: Spheroidal Graphite Iron (SGI) and Compacted Graphite Iron (CGI). SGI is largely known, both at the scientific levels and industrial use. Besides, CGI is a relatively unused and unknown material since its mechanical proprieties are positioned in the middle between the excellent SGI and the less performing white, grey and malleable iron. Respect to these more traditional cast irons, the production of CGI presents higher cost and more difficulties. At the same time CGI could represent the perfect choice respect to specific technical needs when SGI is not applicable while the all other cast irons presents resistances too low. During this investigation, standard test methods were used for the determination of fracture toughness ( $K_{IC}$ ) and plastic-elastic energy ( $J_{IC}$ ) required to grow a crack in these alloys. It was realized under predominantly linear-elastic, plane-strain conditions using fatigue precracked specimens. Experimental values of  $K_{IC}$  and  $J_{IC}$  can be used to the design of structures to ensure that a cast does not fail by brittle or ductile fracture. Adding, comparing data of tests performed over different lots of production, it was possible to estimate the variability of material proprieties related to intrinsic factors of processing. In particular, against the common opinion, it was demonstrated that CGI can be produced with a reasonable level of predictability, higher than the case of SGI.

## Acknowledgement

This investigation was realized thanks to the technical support and financial contribution of SCM Group. In particular, all specimens in SGI and CGI were realized inside the SCM sand casting foundry [34] located in Rimini, Italy.

## REFERENCES

- [1] J.F. Shackelford and A. William (Ed.), *CRC Materials science and engineering handbook*, CRC press, 2000.
- [2] F.C. Campbell. *Elements of Metallurgy and Engineering Alloys*. Materials Park, Ohio, ASM International, 2008.
- [3] H.T. Angus, *Cast iron: physical and engineering properties*. Elsevier, 2013.
- [4] R. Elliott, *Cast iron technology*. Butterworth-Heinemann, 1988.
- [5] ASM. *Speciality handbook: cast irons*. United States: ASM International, pp. 33-267, 1996.
- [6] S. Lampman, 'Fatigue and fracture properties of cast irons.' *ASM International*, Member/Customer Service Center, Materials Park, OH 44073-0002, USA, pp. 665-679, 1996.
- [7] P. Baicchi, L. Collini, and E. Riva, 'A methodology for the fatigue design of notched castings in grey cast iron', *Engineering Fracture Mechanics*, vol. 74, no. 4, pp. 539-548, 2007.
- [8] N.S. Tiedje, 'Solidification, processing and properties of ductile cast iron', *Materials Science and Technology*, vol. 26, no. 5, pp. 505-514, 2010.
- [9] C. Labrecque and M. Gagne, 'Ductile iron: fifty years of continuous development', *Canadian Metallurgical Quarterly*, vol. 37, no. 5, pp. 343-378, 1998.
- [10] N. Fatahalla, S. Bahi, and O. Hussein, 'Metallurgical parameters, mechanical properties and machinability of ductile cast iron', *Journal of Materials Science*, vol. 31, no. 21, pp: 5765-5772, 1996.
- [11] M.N. James and Li Wenfong, 'Fatigue crack growth in austempered ductile and grey cast irons—stress ratio effects in air and mine water', *Materials Science and Engineering*, vol. 265, no. 1 pp. 129-139, 1999.
- [12] P. Clement, J. Pl Angeli, and A. Pineau. 'Short crack behaviour in nodular cast iron', *Fatigue & Fracture of Engineering Materials & Structures* vol. 7, no. 4, pp. 251-265, 1984.
- [13] S. Dawson and T. Schroeder, *Compacted Graphite Iron – A Viable Alternative. Engineered Casting Solutions*, in *AFS Translation*, Spring 2000.
- [14] F. Mocellin, E. Melleras, W.L. Guesser and L. Boehs, 'Study of the Machinability of Compacted Graphite Iron for Drilling Process', *Journal of the Brazilian Society of Mechanical Sciences and Engineering*, vol. 26, no. 1, pp. 22-27, 2004.
- [15] S. Dawson and T. Schroeder, 'Practical applications for compacted graphite iron', *AFS Transactions*, vol. 47, no. 5 pp. 1-9, 2004.
- [16] N. Radović, A. Morri and C. Fragassa, 'A study on the tensile behaviour of spheroidal and compacted graphite cast irons based on microstructural analysis', *11th IMEKO TC15 Youth Symposium on Experimental Solid Mechanics*, 30.05-02.06.2012, Brasov, Romania. pp. 185-190.

- [17] C. Fragassa, N. Radovic, A. Pavlovic and G. Minak, 'Comparison of mechanical proprieties in compacted and spheroidal graphite irons', *Tribology in Industry*, vol. 38, no. 1, pp. 45-56, 2016.
- [18] V.I. Semenov, S.J. Huang, L.Sh. Shuster and P.C. Lin, 'Influence of Microstructure, Produced by Heat Treatment and Sever Plastic Deformation, on Tribological Properties of Low-carbon Steel', *Tribology in Industry*, vol. 33, no. 2, pp. 63-71, 2011.
- [19] D.G. Mallapur and K.R. Udupa, 'A Comparative Study on Wear Properties of As Cast, Cast Aged and Forge Aged A356 Alloy with Addition of Grain Refiner and/or Modifier', *Tribology in Industry*, vol. 37, no. 1, pp. 81-87, 2015.
- [20] B. Bobic, S. Mitrovic, M. Babic, A. Vencl and I. Bobic, 'Corrosion Behavior of the As-cast and Heat-treated ZA27 Alloy', *Tribology in Industry*, vol. 33, no. 2, pp. 87-93, 2011.
- [21] P.J. Emerson and W. Simmons: Final Report on the Evaluation of the Graphite Form in Ferritic Ductile Iron by Ultrasonic and Sonic Testing, and the Effect of Graphite Form on Mechanical Properties. In: *AFS Trans*, no. 76-26, pp. 109-128, 1976.
- [22] B.I. Imasogie, A.A. Afonja and J.A. Ali: Properties of Ductile Iron Nodularised with Multiple Calcium-Magnesium Based Master Alloy. In: *Mater. Sci. And Technology*, 2000, vol. 16, pp. 194-201.
- [23] A.G. Fuller, P.J. Emerson and G.F. Sergeant, 'A Report on the Effect Upon Mechanical Properties of Variation in Graphite Form in Irons Having Varying Amounts of Ferrite and Pearlite in the Matrix Structure and the Use of Nondestructive Tests in the Assessments of Mechanical Properties of such Irons', In: *AFS Trans*, vol. 80, no. 09, pp. 21-50, 1980.
- [24] E. Roy, *Cast iron technology*. London: Butterworth-Heinemann, 1988.
- [25] I. Minkoff, *The physical metallurgy of cast iron*. New York: Wiley, 1983.
- [26] ASTM A247-10, *Standard Test Method for Evaluating the Microstructure of Graphite in Iron Castings*, 2010.
- [27] ASTM E399-12e3, *Standard Test Method for Linear-Elastic Plane-Strain Fracture Toughness  $K_{Ic}$  of Metallic Materials*, 2012.
- [28] ASTM E1820-15, *Standard Test Method for Measurement of Fracture Toughness*, 2015.
- [29] T.L. Anderson. *Fracture mechanics: fundamentals and applications*. CRC press, 2005.
- [30] ASTM E813-89E01, *Test Method for JIC, A Measure of Fracture Toughness* (Withdrawn 1997), 1989.
- [31] P. Clement, J. Pl. Angeli and A. Pineau, 'Short crack behaviour in nodular cast iron', *Fatigue & Fracture of Engineering Materials & Structures*, vol. 7, no. 4, pp. 251-265, 1984.
- [32] S.C. Lee and J. M. Suen: Ultrasonic ND Evaluation of Matrix Structures and Nodularity in Cast Irons. In: *Met. Trans. A.*, vol. 20A, pp. 2399-2407, 1989.
- [33] Z.R. He, G.X. Lin and S.Ji. 'Deformation and fracture of cast iron with an optimized microstructure', *Materials characterization*, vol. 38, no. 4, pp. 251-258, 1997.
- [34] SCM Foundry, available at: <http://www.scmfonderie.it/?l=en&p=azienda>, accessed: 15.11.2015.